Inventory of Supplemental Materials

Diminished MTORC1-Dependent JNK-Activation Underlies the Neurodevelopmental Defects Associated with Lysosomal Dysfunction

Ching-On Wong, Michela Palmieri, Jiaxing Li, Dmitry Akhmedov, Yufang Chao, Geoffrey T. Broadhead, Michael X. Zhu, Rebecca Berdeaux, Catherine A. Collins, Marco Sardiello, and Kartik Venkatachalam

SUPPLEMENTAL MATERIALS

Supplemental Experimental Procedures

Drosophila strains

The wild-type *Drosophila* strains used in the study were *Canton S* and w^{1118}. The *trpml* related strains used were: $trpml^{1}$, $trpml^{2}$, *UAS-trpml*, P[$trpml^{+}$], and Df^{trpml} (*Df(3L)Exel6135*) (all from (Venkatachalam et al., 2008)) and *UAS-trpml::myc* (Wong et al., 2012). Other *Drosophila* strains used in this study were *UAS-spinster::gfp* (Sweeney and Davis, 2002), *UAS-lamp::gfp* (Pulipparacharuvil et al., 2005), *elav-GAL4* (Lin and Goodman, 1994), *C164-GAL4* (Brand and Perrimon, 1993), *mef2-GAL4* (Ranganayakulu et al., 1996), *cg-GAL4* (Hennig et al., 2006), $ragC^{\Delta}$ (Kim et al., 2008), *UAS-*$ragA^{TN}$ (Kim et al., 2008), *UAS-*$ragA^{QL}$ (Kim et al., 2008), *n-syb-GAL4* (Pauli et al., 2008), P{*TRiP.JF01088*} (*UAS-*$raptor^{IR}$) (Bloomington *Drosophila* Stock Center) (Kockel et al., 2010; Lee and Chung, 2007; Natarajan et al., 2013), *vglut*^{ok371}*-GAL4* (*ok371-GAL4*) (Brand and Perrimon, 1993; Meyer and Aberle, 2006), *UAS-*$S6K^{KQ}$ (Barcelo and Stewart, 2002), *UAS-thor* (Bloomington *Drosophila* Stock Center), bsk^{1} (Sluss et al., 1996), wnd^{3} (Collins et al., 2006), *UAS-hiw* (Wu et al., 2005), hiw^{ND8} (Wan et al., 2000), *UAS-rheb* (Stocker et al., 2003), *puc-LacZ* (Martin-Blanco et al., 1998), *BG380-GAL4* (Budnik, 1996), and P{*TRiP.HMS01476*} (*UAS-*$cln3^{IR}$) (Bloomington *Drosophila* Stock Center).

Fly husbandry and chemical feeding

All flies were reared at room temperature (~22°C). Except for the experiments with ML-SA1, yeast, or CH5424802 feeding, all flies were raised in standard fly food (1 L of food contained: 95 g agar, 275 g Brewer's yeast, 520 g of cornmeal, 110 g of sugar, 45 g of

propionic acid, and 36 g of Tegosept). For the drug-feeding experiments, the food was comprised of 1.25 g of instant fly food (formula 4-24 plain, Carolina Biological Supply Company) with 0.125 g of inactive yeast suspended in 3 mL water. For chloroquine feeding experiments, 2 mM chloroquine was added to the food. For ML-SA1 feeding experiments, 20 μM ML-SA1 or 0.1% DMSO was added to the food suspension. For CH5424802 feeding experiments, 1 μM CH5424802 or 0.02% DMSO in 0.5 mL water was added to the fly food on day 5 after egg deposition. Subsequently, an additional 0.5 mL water or 0.5 mL yeast paste (40% w/v) containing CH5424802 (1 μM) or DMSO (0.02%) was laid on top of the fly food.

Image acquisition and quantification

Confocal images of *Drosophila* samples were acquired using a Nikon A1 Confocal Laser Microscope System (Nikon) as Z-series at 1 μm steps. For NMJ bouton number quantification, a 60x oil-immersion objective was used to focus on the NMJ (muscle 6/7, A3 segment). Only type 1 boutons with both HRP- and DLG-positive signals were counted. To isolate the pMAD and Wg signals within the NMJ, masks were applied to eliminate the pMAD and Wg signal outside the DLG-positive regions using Image Pro Plus (Media Cybernetics). Eps15 staining was used in these experiments as a control for antibody staining.

For analysis of expression from *puc*-lacZ reporter, images of larval VNCs were obtained on an Improvision spinning disk confocal microscope (Perkin Elmer), using a 40x oil-immersion objective and 0.8 μm steps. The MN cell bodies along the dorsal midline of the nerve cord in segments A2-A5 were identified based on P-Smad1/5

staining, and Volocity software (Perkin Elmer) was used to measure the mean intensities of β-gal staining in these nuclei. The mean intensity in these MNs per animal was measured for at least 4 animals per genotype, and normalized to *puc-lacZ* expression in controls that were processed in parallel for immunocytochemistry and imaging.

Immunohistochemical images of mouse brain tissues were acquired on a Leica DM RXA2 microscope with Hitachi HVC20A camera, and confocal images of mouse brain tissues were acquired on a Zeiss LSM 710 microscope.

Protein purification

Drosophila Wnd cDNA was sub-cloned into pGEX-KG expression vector. The codon encoding lysine^{188} was mutated to encode an alanine (K188A) to yield GST-tagged Wnd^{KD}. To mutate the putative MTORC1 target sites on Wnd^{KD}, the codons encoding serine^{305}, threonine^{309}, serine^{362}, and serine^{392} were all mutated to encode alanines. The resulting construct was named mut-Wnd^{KD}. The expression constructs were then transformed into BL21-CodonPlus competent *E. coli* cells (Stratagene). IPTG was added to the *E. coli* culture to induce protein expression at 30°C. Total protein was harvested by sonication. The recombinant GST-tagged proteins were purified using glutathione sepharose (GE Life Sciences).

The MTORC1 complex was purified from HEK293T cells stably expressing FLAG-tagged Raptor (FLAG-Raptor) using anti-FLAG M2 Agarose (Sigma-Aldrich). The procedures were followed as described (Yip et al., 2010), except the gel filtration step. The input, flow-through, wash, and eluate fractions were analyzed by SDS-PAGE and

Western blot with anti-MTOR (Cell Signaling), anti-FLAG (Cell Signaling), anti-ULK1 (Cell Signaling), anti-JNK (Santa Cruz), and anti-α-tubulin (DSHB). Eluate fraction 2 (Figure S3) was used for the *in vitro* kinase assay.

Statistical Analysis

Figure 1H Number of boutons: WT (w^{1118}) = 66.7±2.1, $trpml^{1}$ = 46.0±2.3, $trpml^{2}$ = 48.3±3.6, $trpml^{1}/trpml^{2}$ = 43.8±2.6, $trpml^{1}/Df^{trpml}$= 42.7±2.9, P[$trpml^{+}$]; $trpml^{1}$ = 64.5±3.5; *, p = $6.3x10^{-14}$, ANOVA; n = 10-30 NMJs per genotype. *UAS-trpml; trpml*^{1} = 49.3±2.1, *elav-GAL4;; trpml*^{1} = 54.6±2.1, *elav>trpml; trpml*^{1} = 72.5±3.1, *C164-GAL4; trpml*^{1} = 53.7±2.1, *C164>trpml; trpml*^{1} = 71.0±2.5, *mef2-GAL4; trpml*^{1} = 50.9±3.4, *mef2>trpml; trpml*^{1} = 50.1±3.5; *, p = $6.3x10^{-14}$, ANOVA; n = 10-34 NMJs per genotype.

Figure 2H Number of boutons: $ragC^{\Delta}$/+ = 78.3±2.9, $ragC^{\Delta}$ = 48.7±2.2, *UAS-ragA*^{TN} = 69.2±2.0, *elav-GAL4* = 83.0±8.8, *elav>ragA*^{TN} = 53.2±4.0, *UAS-ragA*^{TN}*; trpml*^{1} = 53.9±1.5, *elav-GAL4;; trpml*^{1} = 54.6±2.1, *elav>ragA*^{TN}*; trpml*^{1} = 51.8±3.3, *UAS-ragA*^{QL}*; trpml*^{1} = 46.5±1.2, *n-syb-GAL4; trpml*^{1} = 49.2±1.7, *n-syb>ragA*^{QL}*; trpml*^{1} = 69.6±3.2, *elav>ragA*^{QL}*; trpml*^{1} = 69.9±3.2, *elav>ragA*^{QL} = 73.5±5.4; *, p = $2.8x10^{-13}$, ANOVA; #, p = $1.2x10^{-4}$, ANOVA; ¶, p = $2.8x10^{-13}$, ANOVA; n = 5-30 NMJs per genotype.

Figure 2I Number of boutons: *ok371-GAL4* = 69.5±4.7, *UAS-raptor*^{IR} = 66.7±2.1, *ok371>raptor*^{IR} = 54.8±3.2, *elav-GAL4* = 83.0±8.8, *elav>raptor*^{IR} = 47.4±2.5; *, p = 0.01, ANOVA; #, p = $6.3x10^{-7}$, ANOVA; n = 8-21 NMJs per genotype.

Figure 2J % *trpml*^{1} adults eclosing: *UAS-ragA*^{QL}*; trpml*^{1} = 21.6±10.0, *elav>ragA*^{QL}*; trpml*^{1} = 81.6±13.6; *, p = 0.006, Student's t-test; n = 5-6 vials per genotype.

Figure 3G Number of boutons: *bsk*^{1}/+ = 80.2±4.7, *trpml*^{1}/+ = 70.3±2.8, *bsk*^{1}/+; *trpml*^{1}/+ = 46.7±3.1, *ragC*$^{\Delta}$ /+ = 78.3±2.9, *bsk*^{1}/ *ragC*$^{\Delta}$ = 43.8±2.9; *, p = 3.2x10^{-7}, ANOVA; #, p = 1.9x10^{-9}, ANOVA; n = 9-20 NMJs per genotype.

Figure 3H Number of boutons: *wnd*^{3}/+ = 68.6±2.7, *trpml*^{1}/+ = 70.3±2.8, *wnd*^{3}/*trpml*^{1} = 47.6±1.1; *, p = 5.9x10-10, ANOVA; n = 10-15 NMJs per genotype.

Figure 3J Number of boutons: ML-SA1 (-): *elav>hiw* = 63±2.8, elav>*hiw; trpml*^{1}/+ = 51.3±2.8, *trpml*^{1} = 50.1±1.6, ML-SA1 (+): *elav>hiw; trpml*^{1}/+ = 66.5±3.7, *trpml*^{1} = 50.2±2.8; *, p = 0.006 and #, p = 0.003, unpaired Student's t-tests; n = 7-18 NMJs per genotype.

Figure 4E Number of boutons: *hiw*^{ND8} = 108.9±3.4, *hiw*^{ND8};; *trpml*^{1} = 70.2±3.6, *hiw*^{ND8}; *UAS-ragA*^{TN} = 100.6±3.9, *hiw*^{ND8}; *ok371-GAL4* = 113.7±5.0, *hiw*^{ND8}; *ok371>ragA*^{TN} = 83.7±4.7, *hiw*^{ND8}; *UAS-raptor*^{IR} = 120±5.2, *hiw*^{ND8}; *ok371>raptor*^{IR} = 100.8±5.6; *, p = 5.1x10^{-10}, unpaired Student's t-test; #, p = 0.001, ANOVA; ¶, p = 0.02, unpaired Student's t-test; n = 6-28 NMJs per genotype.

Figure 4J Number of boutons: *UAS-rheb* = 54.8±3.3, *elav>rheb* = 121.8±9.9, *UAS-rheb, wnd*^{3}/+ = 59.2±2.4, *elav-GAL4; wnd*^{3}/+ = 67.1±4.0, *elav>rheb; wnd*^{3}/+ = 80.4±4.8; *, p = 1.9x10^{-6}, unpaired Student's t-test; #, p = 2.7x10^{-4}, unpaired Student's t-test; n = 8-18 NMJs per genotype.

Figure 5B Relative pJNK intensities (normalized to WT values): *ragC*$^{\Delta}$ = 0.64±0.08, *hiw*^{ND8} = 1.5±0.2, *hiw*^{ND8}*;; trpml*^{1} = 1.2±0.1; *, p = 0.001, unpaired Student's t-test; ¶, p = 0.01; #, p = 0.04, unpaired Student's t-tests, n = 5-7 separate samples per genotype.

Figure 5C Relative JNK intensities: *ragC*$^{\Delta}$ *normalized to* WT = 0.95±0.03, *hiw*^{ND8}*;; trpml*^{1} normalized to *hiw*^{ND8} = 1.15±0.19; n = 4-6 separate samples per genotype.

Figure 5D Relative pJNK/JNK intensities: *elav>rheb* normalized to *UAS-rheb* = 1.24±0.06; *, p = 0.005, paired Student's t-test; n = 8 samples per genotype.

Figure 5F Relative β-Gal intensities (normalized to *BG380-GAL4/+* mean): *BG380-GAL4/+* = 1±0.05, *BG380>ragA*^{TN} = 0.8±0.02, *BG380>raptor*^{IR} =0.8±0.01; *, p = 0.009, ANOVA; n = 3-4 animals per genotype.

Figure 5G Relative β-GAL intensities (normalized to *BG380-GAL4/+* mean): *BG380-GAL4/+* = 1±0.02, *BG380>rheb* = 2.6±0.5; *, p<0.003, Student's t-test; n = 7 animals per genotype.

Figure 5I Relative Wnd phosphorylation (normalized to control): GST-Wnd^{KD}: 10 μM Torin1 = 0.7±0.06; *, p = 0.0013, paired Student's t-test, n = 8; GST-mut-Wnd^{KD}: 10 μM Torin1 = 1±0.3, n = 3.

Figure 6C Number of boutons: *cln3*$^{\Delta MB1}$*/+* = 65.3±2.4, *cln3*$^{\Delta MB1}$ = 44.8±1.8, *UAS-cln3*^{IR} = 76.1±2.9, *ok371-GAL4* = 69.5±4.7, *ok371>cln3*^{IR} = 48.1±2.5; *, p = 1.5x10^{-5}, Student's t-test; #, p = 2.1x10^{-7}, ANOVA; n = 7-17 NMJs per genotype.

Figure 6D Number of boutons: *cln3*$^{\Delta MB1}$*/+* = 65.3±2.4, *trpml*^{1}*/+* = 70.3±2.8, *cln3*$^{\Delta MB1}$*/trpml*^{1} = 44.5±2.1, *UAS-ragA*^{QL}*;cln3*$^{\Delta MB1}$ = 41.2±2.2, *elav>ragA*^{QL}*;cln3*$^{\Delta MB1}$ =

69.0±4.0, *elav>ragA*^{QL} = 73.5±5.4; *, p = 1.5x10^{-8}, ANOVA; #, p = 2.7x10^{-5}, Student's t-test; n = 7-15 NMJs per genotype.

Figure 6F Relative pJNK intensities: *n-syb>cln3*^{IR} normalized to *UAS-cln3*^{IR} = 0.67±0.002; *, p = 3x10^{-5}, paired Student's t-tests, n = 3 separate samples per genotype.

Figure 6N Relative pJNK/GAPDH intensities (normalized to WT mean): WT = 1±0.02, *Cln3*$^{-/-}$ = 0.46±0.03; *, p = 0.002, paired Student's t-tests, n = 3 separate samples per genotype.

Figure 6O Relative pJNK/JNK intensities (normalized to WT mean): WT = 1±0.05, *Cln3*$^{-/-}$ = 0.57±0.02; *, p = 0.01, Student's t-tests, n = 3 separate samples per genotype.

Figure 7A Number of boutons: Yeast (-): WT = 81.0±6.4, *trpml*^{1} = 55.0±2.4; Yeast (+): *trpml*^{1} = 59.5±3.9; n = 11-14 NMJs per genotype.

Figure 7C-D Number of boutons: Yeast (-) & CH5424802 (-): *trpml*^{1} = 54.9±2.3, *elav>ragA*^{TN};*trpml*^{1} = 46.6±2.2, WT =85.1±3.5 ,*ragC* ˙ = 56.4±1.9; Yeast (+) & CH5424802 (-): *trpml*^{1} = 54.3±1.8, *elav>ragA*^{TN};*trpml*^{1} = 45±2.1, *ragC* ˙ = 59.2±2.7; Yeast (-) & CH5424802 (+): *trpml*^{1} = 51.8±2.9, *elav>ragA*^{TN};*trpml*^{1} = 48.8±2; Yeast (+) & CH5424802 (+): *trpml*^{1} = 66.2±2.0, *elav>ragA*^{TN};*trpml*^{1} = 47.3±2.5, *ragC* ˙ = 52.9±2.6; *, p = 1.1x10^{-5}, ANOVA; n = 20-32 NMJs per genotype.

Figure 7E Number of boutons in *UAS-cln3*^{IR}: Yeast (-) & CH5424802 (-) = 72.4±1.9; Number of boutons in *ok>cln3*^{IR}: Yeast (-) & CH5424802 (-) = 45.0±1.9; Yeast (+) & CH5424802 (-) = 36.5±4.3; Yeast (+) & CH5424802 (+) = 57.3±2.2; *, p = 6.6x10^{-12}, unpaired Student's t-test; #, p = 7x10^{-5}, ANOVA; n = 14-19 NMJs per genotype.

Figure 7F % adults eclosing: Yeast (+) & CH5424802 (-) = 46.1±4.9; Yeast (+) & CH5424802 (+) = 63.2±2.3; *, p = 0.03, unpaired Student's t-test; n = 4 vials per treatment.

Figure S1C Number of boutons: WT = 66.7±2.1, *elav>ampk*^{T184D} = 43.9±3.1, *trpml*^{1} = 46.0±2.3, *elav>ampk*^{T184D}*;trpml*^{1} = 46.4±1.7, *UAS-ampk*^{K56R}*;trpml*^{1} = 46.3±2.1, *elav>ampk*^{K56R}*;trpml*^{1} = 53.4±3.3; *, p =3.3x10^{-14}, ANOVA; n = 10-18 NMJs per genotype.

Figure S1D Number of boutons: *UAS-S6K*^{KQ} = 65.1±2.2, *elav>S6K*^{KQ} = 68.4±5.0, *UAS-thor* = 61.6±1.9, *elav>thor* = 66.2±2.8; n = 8-16 NMJs per genotype.

Figure S1E Number of boutons: DMSO control = 70.5±4.4, 1 µM rapamycin = 78.2±4.8; n = 10-12 NMJs per genotype.

Figure S1B Relative pMAD intensities (normalized to WT mean): WT = 1±0.02, *trpml*^{1} = 0.75±0.1; p = 0.09, unpaired Student's t-test, n = 5-6 NMJs per genotype.

Figure S1D Relative pMAD intensities (normalized to WT mean): WT = 1±0.09, *trpml*^{1} = 1.2±0.13; n = 4 animals per genotype.

Figure S1E Relative Wg intensities (normalized to WT mean): WT = 1±0.2, *trpml*^{1} = 1.1±0.35; n = 3-6 NMJs per genotype.

Figure S4B Relative pJNK/JNK levels: control = 1±0.004, chloroquine fed larvae = 0.69±0.09; *, p = 0.04, unpaired Student's t-test, n = 3 independent samples per condition.

Figure S4G Number of boutons: *hiw*^{ND8}*; UAS-cln3*^{IR} = 113.5±4.8, *hiw*^{ND8}*; ok371-GAL4* = 113.7±5.0, *hiw*^{ND8}*; ok371>cln3*^{IR} = 95.5±3.4; *, p = 0.02, ANOVA; n = 6-19 NMJs per genotype.

Figure S4M Relative pAkt^{S473} levels normalized to control: CH5424802 treated larvae = 0.8±0.05; *, p = 0.01, paired Student's t-test, n = 5 pairs of independent samples per condition.

Supplemental References

Barcelo, H., and Stewart, M.J. (2002). Altering Drosophila S6 kinase activity is consistent with a role for S6 kinase in growth. Genesis *34*, 83-85.

Brand, A.H., and Perrimon, N. (1993). Targeted gene expression as a means of altering cell fates and generating dominant phenotypes. Development *118*, 401-415.

Budnik, V. (1996). Synapse maturation and structural plasticity at Drosophila neuromuscular junctions. Curr Opin Neurobiol *6*, 858-867.

Collins, C.A., Wairkar, Y.P., Johnson, S.L., and DiAntonio, A. (2006). Highwire restrains synaptic growth by attenuating a MAP kinase signal. Neuron *51*, 57-69.

Hennig, K.M., Colombani, J., and Neufeld, T.P. (2006). TOR coordinates bulk and targeted endocytosis in the *Drosophila melanogaster* fat body to regulate cell growth. J Cell Biol *173*, 963-974.

Kim, E., Goraksha-Hicks, P., Li, L., Neufeld, T.P., and Guan, K.L. (2008). Regulation of TORC1 by Rag GTPases in nutrient response. Nat Cell Biol *10*, 935-945.

Kockel, L., Kerr, K.S., Melnick, M., Bruckner, K., Hebrok, M., and Perrimon, N. (2010). Dynamic switch of negative feedback regulation in Drosophila Akt-TOR signaling. PLoS Genet *6*, e1000990.

Lee, G., and Chung, J. (2007). Discrete functions of rictor and raptor in cell growth regulation in Drosophila. Biochem Biophys Res Commun *357*, 1154-1159.

Lin, D.M., and Goodman, C.S. (1994). Ectopic and increased expression of Fasciclin II alters motoneuron growth cone guidance. Neuron *13*, 507-523.

Martin-Blanco, E., Gampel, A., Ring, J., Virdee, K., Kirov, N., Tolkovsky, A.M., and Martinez-Arias, A. (1998). puckered encodes a phosphatase that mediates a feedback loop regulating JNK activity during dorsal closure in Drosophila. Genes Dev *12*, 557-570.

Meyer, F., and Aberle, H. (2006). At the next stop sign turn right: the metalloprotease Tolloid-related 1 controls defasciculation of motor axons in Drosophila. Development *133*, 4035-4044.

Natarajan, R., Trivedi-Vyas, D., and Wairkar, Y.P. (2013). Tuberous sclerosis complex regulates Drosophila neuromuscular junction growth via the TORC2/Akt pathway. Hum Mol Genet *22*, 2010-2023.

Pauli, A., Althoff, F., Oliveira, R.A., Heidmann, S., Schuldiner, O., Lehner, C.F., Dickson, B.J., and Nasmyth, K. (2008). Cell-type-specific TEV protease cleavage reveals cohesin functions in Drosophila neurons. Dev Cell *14*, 239-251.

Pulipparacharuvil, S., Akbar, M.A., Ray, S., Sevrioukov, E.A., Haberman, A.S., Rohrer, J., and Krämer, H. (2005). *Drosophila* Vps16A is required for trafficking to lysosomes and biogenesis of pigment granules. J Cell Sci *118*, 3663-3673.

Ranganayakulu, G., Schulz, R.A., and Olson, E.N. (1996). Wingless signaling induces nautilus expression in the ventral mesoderm of the Drosophila embryo. Dev Biol *176*, 143-148.

Sluss, H.K., Han, Z., Barrett, T., Goberdhan, D.C., Wilson, C., Davis, R.J., and Ip, Y.T. (1996). A JNK signal transduction pathway that mediates morphogenesis and an immune response in Drosophila. Genes Dev *10*, 2745-2758.

Stocker, H., Radimerski, T., Schindelholz, B., Wittwer, F., Belawat, P., Daram, P., Breuer, S., Thomas, G., and Hafen, E. (2003). Rheb is an essential regulator of S6K in controlling cell growth in Drosophila. Nat Cell Biol *5*, 559-565.

Sweeney, S.T., and Davis, G.W. (2002). Unrestricted synaptic growth in *spinster*-a late endosomal protein implicated in TGF-β-mediated synaptic growth regulation. Neuron *36*, 403-416.

Venkatachalam, K., Long, A.A., Elsaesser, R., Nikolaeva, D., Broadie, K., and Montell, C. (2008). Motor deficit in a *Drosophila* model of mucolipidosis type IV due to defective clearance of apoptotic cells. Cell *135*, 838-851.

Wan, H.I., DiAntonio, A., Fetter, R.D., Bergstrom, K., Strauss, R., and Goodman, C.S. (2000). Highwire regulates synaptic growth in Drosophila. Neuron *26*, 313-329.

Wong, C.O., Li, R., Montell, C., and Venkatachalam, K. (2012). Drosophila TRPML Is Required for TORC1 Activation. Curr Biol *22*, 1616-1621.

Wu, C., Wairkar, Y.P., Collins, C.A., and DiAntonio, A. (2005). Highwire function at the Drosophila neuromuscular junction: spatial, structural, and temporal requirements. J Neurosci *25*, 9557-9566.

Yip, C.K., Murata, K., Walz, T., Sabatini, D.M., and Kang, S.A. (2010). Structure of the human mTOR complex I and its implications for rapamycin inhibition. Mol Cell *38*, 768-774.

Figure S1 (related to Figure 2)

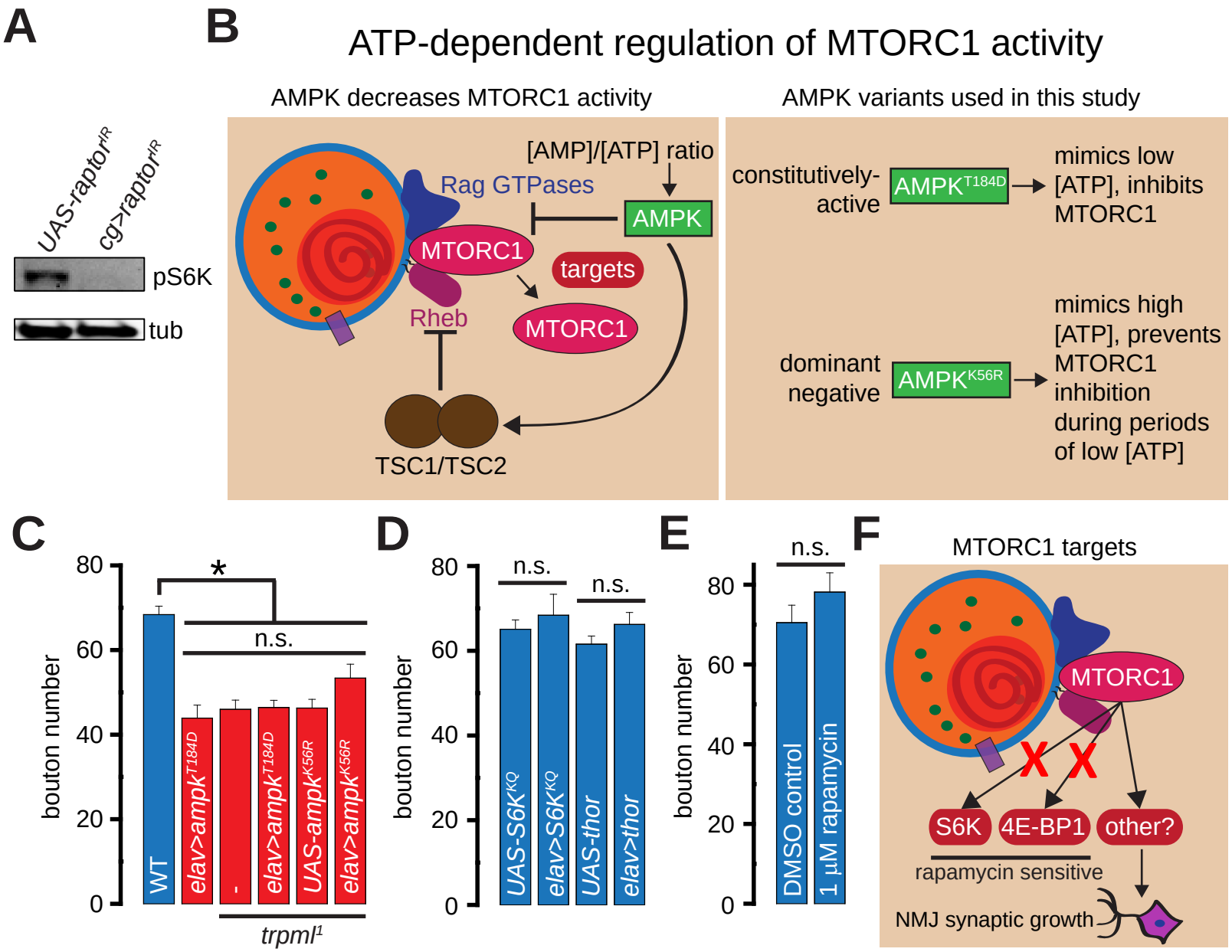

Figure S1. Synaptic growth defects following lysosomal dysfunction do not arise from elevated AMPK activity or diminished phosphorylation of S6K/Thor.

(A) Western blots performed *Drosophila* 3rd instar larval fat-body from animals of the indicated genotypes probed with α-pS6K and α-tubulin primary antibodies.

(B) Schematic diagram showing the role of AMPK in regulating MTORC1 activity and the AMPK variants used in this study.

(C-D) Bar graphs showing the average bouton numbers in animals of the indicated genotypes.

(E) Bar graph showing the average number of boutons in wild-type larvae reared on instant food containing the indicated drugs.

(F) Schematic showing that MTORC1 regulates NMJ synaptic growth via targets other than S6K and 4E-BP1.

All values represent mean ±SEM, and "*" represents statistical significance. Please consult the *Supporting Information* for all values and information on statistical tests employed. Abbreviations: n.s., not significant.

Figure S2 (related to Figure 3)

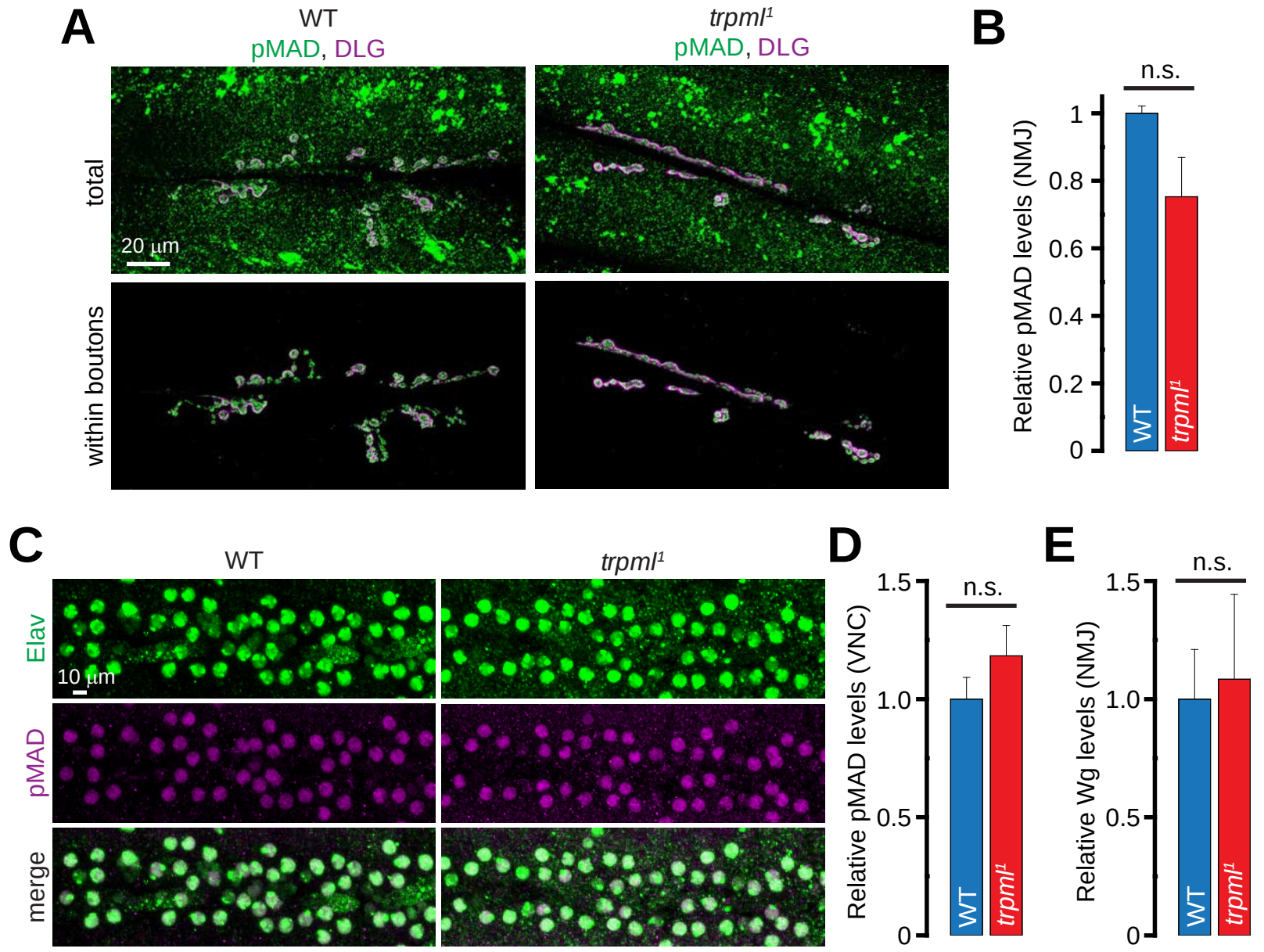

Figure S2. Synaptic growth defects following lysosomal dysfunction do not arise from alterations in BMP/TGF-β signaling or Wg release.

(A) Confocal images of 3rd instar larval NMJs from animals of the indicated genotypes stained with antibodies against pMAD (green) and DLG (magenta). Scale bar shown in top-left panel also applies to remaining panels. Please refer to the *Experimental Procedures* for information on the approach utilized to isolate the pMAD signal within boutons.

(B) Bar graph showing the relative pMAD intensities normalized to the Eps15 intensities within NMJ boutons in animals of the indicated genotypes. All values were normalized to the Eps15 staining intensities.

(C) Confocal images of 3rd instar larval VNC from animals of the indicated genotypes stained with antibodies against pMAD (magenta) and Elav (green). Scale bar shown in top-left panel also applies to remaining panels.

(D) Bar graph showing the relative pMAD intensities normalized to the Elav intensities within VNC in animals of the indicated genotypes.

(E) Bar graphs showing the relative Wg intensities normalized to the Eps15 intensities within NMJ boutons in animals of the indicated genotypes. All values were normalized to the Eps15 staining intensities. Please refer to the *Experimental Procedures* for information on the approach utilized to isolate the Wg signal within boutons.

All values represent mean ±SEM. Please consult the *Supporting Information* for all values and information on statistical tests employed. Abbreviations: n.s., not significant.

Figure S3 (related to Figure 5)

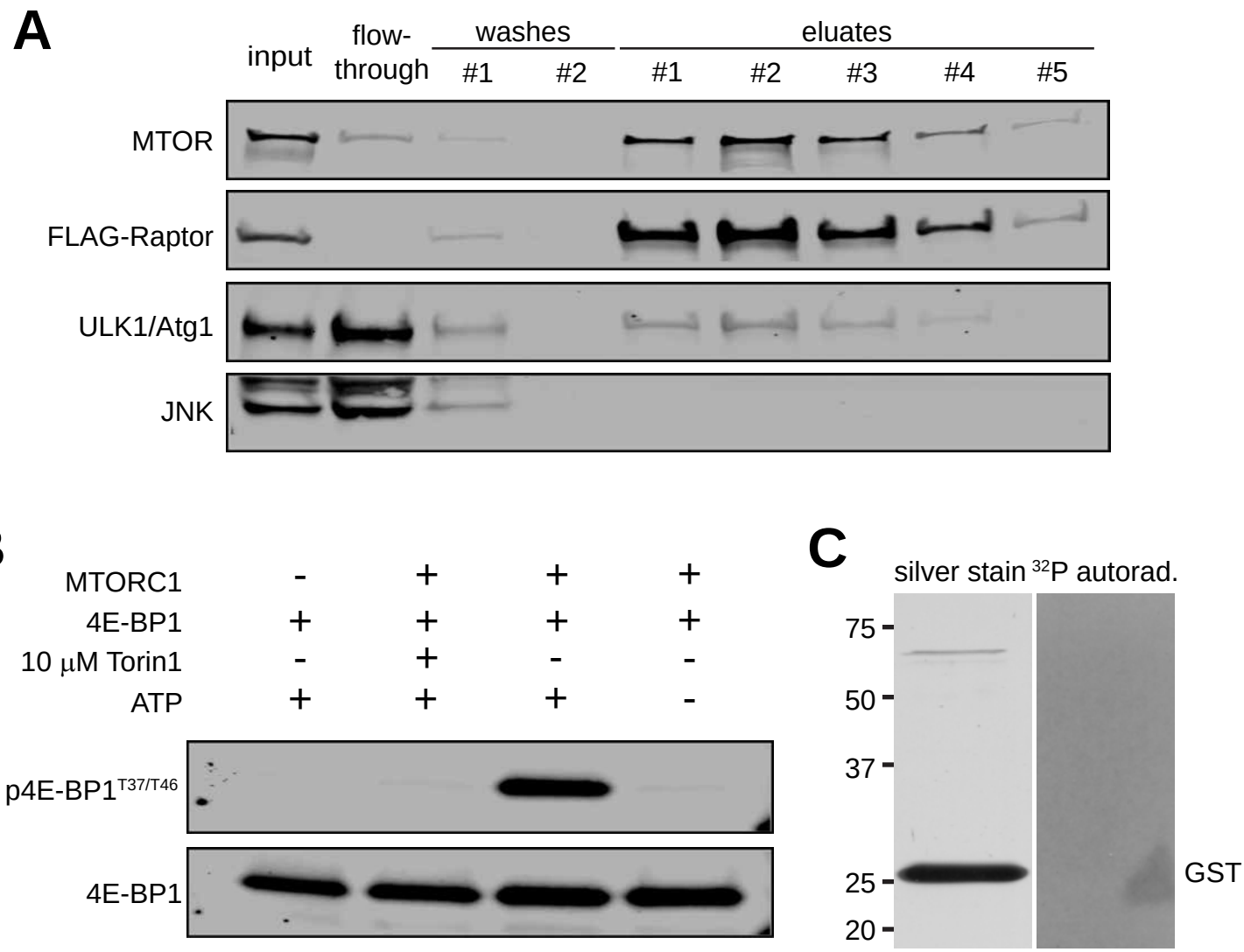

Figure S3. Characterization of purified MTORC1

(A) Western blot performed on the indicated fractions from the FLAG-Raptor purification probed with antibodies against MTOR, FLAG, ULK1/Atg1 and JNK.

(B) *In vitro* kinase assay using purified MTORC1 on recombinant 4E-BP1. Upper panel shows that 4E-BP1 is phosphorylated only in the presence of MTORC1 and ATP, and this phosphorylation of 4E-BP1 is inhibited by 10 μM Torin1. Lower panel shows total 4E-BP1 in all the lanes.

(C) *In vitro* kinase assay using purified MTORC1 on recombinant GST. Left panel, silver stain showing the presence of GST. Right panel, ^{32}P autoradiogram showing that GST is not phosphorylated by MTORC1.

Figure S4 (related to Figures 6 and 7)

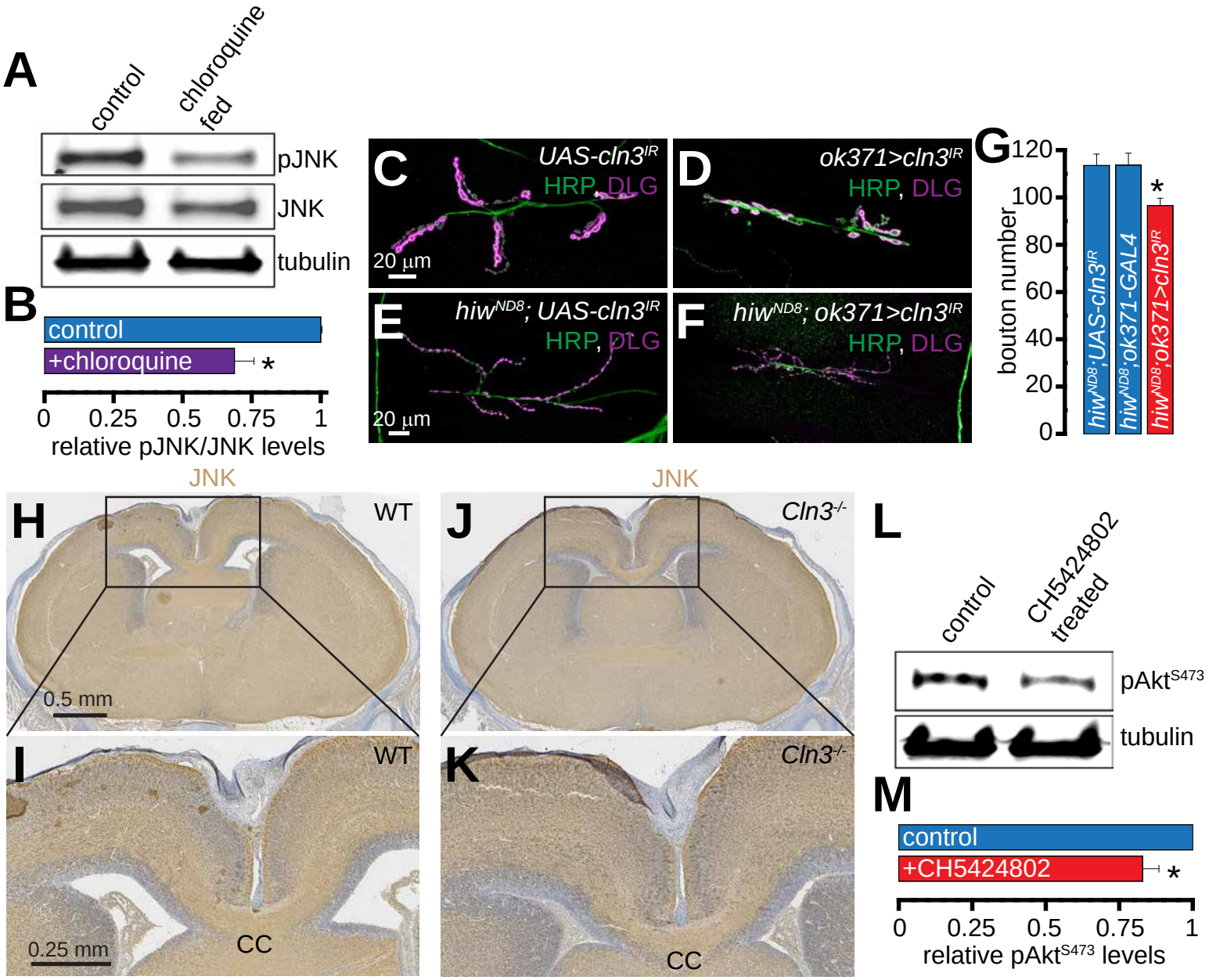

Figure S4.

(A) Western blots performed on 3rd instar larval brain extracts derived from control or choloroquine fed larvae probed with α-pJNK, α-JNK, and α-tubulin primary antibodies.

(B) Bar graph showing the relative pJNK/JNK levels in 3rd instar larval brain extracts derived from control or choloroquine fed larvae.

(C-F) Confocal images of 3rd instar larval NMJs from animals of the indicated genotypes stained with antibodies against HRP (green) and DLG (magenta). Scale bar shown in (C) and (E) also apply to (D) and (F) respectively.

(G) Bar graph showing the average bouton numbers in animals of the indicated genotypes.

(H and J) Coronal sections of E19.5 mouse brains of the indicated genotypes showing α-JNK staining by immunohistochemistry. Scale bar shown in (F) also applies to (H).

(Iand K) Higher magnification of the boxed regions from (F) and (H) respectively.

(L) Western blots performed on 3rd instar larval brain extracts derived from tissues treated with DMSO (control) or CH5424802 probed with α-pAkt^{S473} and α-tubulin primary antibodies.

(M) Bar graph showing the relative pAktS^{473} levels in 3rd instar larval brain extracts derived from tissues treated with DMSO (control) or CH5424802 (1 μM) for 1 hour.

All values represent mean ±SEM, and "*" represents statistical significance. Please consult the *Supporting Information* for all values and information on statistical tests employed. Abbreviations: CC, corpus callosum.